Development 136, 4143-4153 (2009) doi:10.1242/dev.043281

Atf4 regulates chondrocyte proliferation and differentiation during endochondral ossification by activating *Ihh* transcription

Weiguang Wang, Na Lian, Lingzhen Li, Heather E. Moss, Weixi Wang, Daniel S. Perrien, Florent Elefteriou and Xiangli Yang*

Activating transcription factor 4 (Atf4) is a leucine-zipper-containing protein of the cAMP response element-binding protein (CREB) family. Ablation of *Atf4* (*Atf4*$^{-/-}$) in mice leads to severe skeletal defects, including delayed ossification and low bone mass, short stature and short limbs. Atf4 is expressed in proliferative and prehypertrophic growth plate chondrocytes, suggesting an autonomous function of Atf4 in chondrocytes during endochondral ossification. In *Atf4*$^{-/-}$ growth plate, the typical columnar structure of proliferative chondrocytes is disturbed. The proliferative zone is shortened, whereas the hypertrophic zone is transiently expanded. The expression of Indian hedgehog (*Ihh*) is markedly decreased, whereas the expression of other chondrocyte marker genes, such as type II collagen (*Col2a1*), PTH/PTHrP receptor (*Pth1r*) and type X collagen (*Col10a1*), is normal. Furthermore, forced expression of Atf4 in chondrocytes induces endogenous *Ihh* mRNA, and Atf4 directly binds to the *Ihh* promoter and activates its transcription. Supporting these findings, reactivation of Hh signaling pharmacologically in mouse limb explants corrects the *Atf4*$^{-/-}$ chondrocyte proliferation and short limb phenotypes. This study thus identifies Atf4 as a novel transcriptional activator of *Ihh* in chondrocytes that paces longitudinal bone growth by controlling growth plate chondrocyte proliferation and differentiation.

KEY WORDS: Atf4, Ihh, Growth plate chondrocytes, Endochondral ossification, Gene transcription, Mouse

INTRODUCTION

The mammalian skeleton is formed through intramembranous and endochondral ossification. The initial step of skeletal development is patterning. At 10 days post-coitum (dpc), during mouse embryogenesis, a group of homogenous cells gives rise to mesenchymal structures and functions in a precise spatial and temporal pattern. Condensation of mesenchymal progenitor cells into a mass that provides the mold of the future skeleton follows this initial patterning (Kaufman, 1992). The condensed mesenchymal cells then differentiate into osteoblasts directly during intramembranous ossification, or into chondrocytes to form the cartilage anlagen, which is eventually replaced by bone during endochondral ossification (Karsenty and Wagner, 2002). Endochondral ossification is crucial for skeletal growth in the developing vertebrate, as well as for skeletal repair in adults. It involves slowly proliferating, rounded, resting chondrocytes in the reserve zone acquiring cues to become rapidly dividing cells that are flattened and packed into columnar chondrocytes in the proliferating zone. Rapidly proliferating chondrocytes then stop dividing to progress to a transition stage of prehypertrophic chondrocytes, which quickly undergo differentiation (hypertrophy). Mature hypertrophic chondrocytes eventually die, allowing vascular invasion, a process that involves the entry of osteoclast and osteoblast precursors. Osteoclasts assist in the removal of cartilage matrix and osteoblasts use the remnants of cartilage matrix as a scaffold for the deposition of new bone matrix to form calcified bone. Therefore, endochondral ossification is a dynamic event that relies on chondrocyte proliferation and differentiation and is tightly regulated by systemic factors, locally secreted factors and transcription factors (reviewed by Day and Yang, 2008; de Crombrugghe et al., 1991; Kronenberg, 2003; Mackie et al., 2008; Nilsson et al., 2005; Ornitz, 2005; Zuscik et al., 2008).

Indian hedgehog (Ihh) belongs to the hedgehog (Hh) family and is one of the aforementioned locally secreted factors required for mammalian skeletal development. By binding to its receptor patched, Hh ligands induce the release of patched inhibition of smoothened, which allows activation of signaling events that promote cell proliferation (Alcedo and Noll, 1997; Day and Yang, 2008). In the growth plate, Ihh is secreted by prehypertrophic chondrocytes and acts as a paracrine factor to promote adjacent chondrocyte proliferation. Ihh can also diffuse and reach cells in the articular perichondrium, where it induces the expression of parathyroid hormone related protein (PTHrP; Pthlh – Mouse Genome Informatics), which in turn inhibits chondrocyte hypertrophy and maintains the pool of proliferative chondrocytes (Chung et al., 2001; Guo et al., 2006; Karp et al., 2000; Minina et al., 2001; St-Jacques et al., 1999). Although the mechanism is not yet fully understood, this action of PTHrP to inhibit hypertrophy forms a negative-feedback regulatory loop on the production of Ihh, which controls the coordination between proliferation and differentiation of participating chondrocytes. Using genetic mouse models, Mak et al. demonstrated that Ihh also promotes chondrocyte hypertrophy in a PTHrP-independent manner (Mak et al., 2008). Given the crucial role that Hh signaling plays in the regulation of skeletal development, it is of interest to understand upstream signaling pathways that regulate *Ihh* at the transcriptional level.

Recent studies have identified several transcription factors that activate *Ihh* transcription. Runx proteins are a group of cell-specific transcription factors belonging to the Runt family (see Karsenty, 2001). Using genetic mouse models, Yoshida et al. found that Runx2, with the assistance of Runx3, binds directly to the *Ihh* promoter and activates its expression (Yoshida et al., 2004). This was the first and thus far only characterization of a transcriptional

Vanderbilt Center for Bone Biology, Vanderbilt University Medical Center, 2215 Garland Avenue, 1225F Medical Research Building IV, Nashville, TN 37232, USA.

*Author for correspondence (xiangli.yang@vanderbilt.edu)

Accepted 6 October 2009

mechanism involved in the regulation of chondrocyte proliferation and hypertrophy in vivo. Msx2, a homeodomain-containing protein that regulates cellular development in many tissues, including bone, teeth and neurons, has been shown to activate *Ihh* transcription in vitro (Amano et al., 2008); however, whether Msx2 is a transcriptional regulator of *Ihh* in vivo remains to be determined.

Atf4 is a leucine-zipper-containing transcription factor of the CREB family (Shaywitz and Greenberg, 1999). Using biochemical and genetic approaches, we have found that inactivation of *Atf4* in mice results in severe osteopenia, which is caused by a failure of *Atf4*$^{-/-}$ osteoblasts to achieve terminal differentiation and to synthesize type I collagen, the main constituent of bone matrix (Yang et al., 2004). In addition, *Atf4*$^{-/-}$ mice display dwarfism, suggesting a role of Atf4 in development of the growth plate chondrocyte. In this study, we identified Atf4 as a direct transcriptional activator of *Ihh* and thus a regulator of chondrocyte proliferation and differentiation.

MATERIALS AND METHODS

Animals

Wild-type (WT) and *Atf4*$^{-/-}$ embryos and mice were obtained by crossing *Atf4*$^{+/-}$ mice. Zero dpc (E0) was defined by the morning the vaginal plug was found. *Atf4* genotyping was performed by PCR using tail DNA (Masuoka and Townes, 2002). For each genotype, at least three embryos or mice were analyzed.

Atf4 expression

Primary chondrocytes were isolated by sequential digestion of rib cage cartilage from E14 embryos with collagenase D. Nuclear extracts isolated from the indicated sources were subjected to western blot analysis using an antibody against Atf4 (N127) (Yang and Karsenty, 2004). Immunohistochemistry was performed on paraffin-embedded sections (5 μm) of WT and *Atf4*$^{-/-}$ humeri. After deparaffinization and rehydration, antigens were retrieved by heating at 100°C for 10 minutes in Tris/EDTA buffer (pH 9.0) and immunostained with antibody N127. Sections were counterstained with Hematoxylin.

Skeletal preparation and histology

Skeletal preparation was according to standard protocols. For histology, embryos and P0 mice were fixed in 4% paraformaldehyde (PFA), embedded in Paraplast, and sectioned at 5 μm. Slides were stained with Hematoxylin for nuclei, Alcian Blue for cartilage matrix, and Alizarin Red for bone matrix.

Microcomputed tomography (μCT) analysis

WT and *Atf4*$^{-/-}$ tibiae were collected and fixed overnight in 4% PFA (pH 7.4) and then 70% ethanol. Samples were scanned using a μCT system (Scanco μCT 40; Bassersdorf, Switzerland). Tomographic cross-sectional images of the proximal tibia were acquired at 55 kV and 145 mA, at an isotropic voxel size of 12 μm and an integration time of 250 milliseconds. Contours were fitted to the outer perimeter of the tibia beginning immediately distal to the growth plate and extending 1.2 mm distally using the auto-contouring feature in the Scanco Software with the threshold of 300 mg hydroxyapatite/cm^3.

In vivo proliferation assay

For embryo limbs, pregnant mice received intraperitoneal injections of 0.1 mg 5-bromo-2′-deoxyuridine (BrdU)/g body weight and were sacrificed 2 hours later. For P0 pups, BrdU (0.1 mg/g body weight) was injected under the skin on the back of the neck 2 hours prior to sacrifice. In organ cultures, BrdU was added 1 hour prior to sample harvesting. Limbs were dissected and fixed in 4% PFA overnight at 4°C. After embedding and sectioning, BrdU was detected with a BrdU Staining Kit (Zymed Laboratories) following the manufacturer's procedure.

TUNEL assay

Apoptotic cells in the growth plate of WT and *Atf4*$^{-/-}$ humeri were detected by in situ terminal deoxynucleotidyltransferase deoxyuridine triphosphate nick end labeling (TUNEL) assay using the In Situ Cell Death Detection Kit (Roche) following the manufacturer's instructions.

In situ hybridization

Alternate sections used for histological analysis were in situ hybridized for chondrocytic marker genes. Probes for type II collagen (*Col2a1*), *Ihh* and type X collagen *Col10a1* were as described previously (Ducy et al., 1997; Takeda et al., 2001). The probe for *PPR* was from Dr T. J. Martin (University of Melbourne, Australia). The probe for *Gli1* was a mouse cDNA fragment (bp 968 to 1437), which was generated by RT-PCR using primers: forward, 5′-GAAGGAATTCGTGTGCCATT-3′ and reverse, 5′-TCCAAGCTGG-ACAAGTCCTC-3′. Antisense cDNAs were used for riboprobe synthesis with RNA polymerases (Invitrogen) and [^{35}S]uridine triphosphate (Perkin Elmer).

Establishment of Atf4-overexpressing chondrocytes

TMC23 chondrocytic cells (Xu et al., 1998) at 90% confluence were transfected with 50 ng Atf4 or Runx2 expression plasmid (pcDNA3.1-Atf4 or pcDNA3.1-Runx2) using Lipofectamine (Invitrogen). When cells reached 100% confluence, they were trypsinized and replated in αMEM containing G418 (400 μg/ml). G418-resistant clones were selected and maintained in G418-containing αMEM.

Electrophoretic mobility shift assay (EMSA)

Oligonucleotides of OSE1 in the osteocalcin gene 2 (*Bglap2*) promoter and of OSE1-like sequences (A1 to A9) in the *Ihh* promoter were synthesized. Annealed double-stranded oligonucleotides were labeled with [^{32}P]dCTP and [^{32}P]ATP and used as probes in EMSA, which was performed as described previously (Ducy and Karsenty, 1995; Schinke and Karsenty, 1999) using purified recombinant Atf4 or nuclear extracts of primary chondrocytes.

Northern hybridization and real-time quantitative RT-PCR (qRT-PCR)

Total RNA was isolated using TRIzol (Invitrogen) and 10 μg from each sample was resolved in a 1% agarose gel, transferred onto nylon membrane, and hybridized with *Ihh*, *PTHrP* or *Gapdh* cDNA probes following standard protocols. qRT-PCR was performed using a standard TaqMan PCR Kit protocol on an Applied Biosystems 7300 machine. After treatment with DNase I, total RNA (2 μg) was reverse-transcribed with reverse transcriptase (Invitrogen) using 100 μM random hexamer primers. Specific oligonucleotide primers were from Applied Biosystems (*Ihh*, Mm00439613 m1; *PTHrP*, Mm00436056_g1; *Gli1*, Mm00494645_m1; *PPR*, Mm00441046_m1).

Construction of an *Ihh* luciferase reporter construct and mutagenesis

A 4.5 kb *Ihh* promoter fragment isolated from a bacterial artificial chromosomal clone, RP24-317G11 (Children's Hospital of Oakland Research Institute, Oakland, CA, USA) was inserted to a luciferase (Luc)-containing reporter vector. A construct containing a 1.3 kb *Ihh* promoter fragment was generated by removal of the 5′ end of the 4.5 kb fragment by restriction digestion. Constructs containing 742 bp and 715 bp *Ihh* promoter fragments were cloned by PCR using the High Fidelity PCR System (Roche) or Pfu DNA polymerase (Stratagene) with the following primer sequences: for the 742 bp fragment, forward 5′-CTGAGAAAGGGAATGTTGCC-3′ and reverse 5′-GCGTGCTGTCCCCCTCGGCG-3′; for the 707 bp fragment, forward 5′-AACTCGAGCACCAGGTTATGAATGACCT-3′ and reverse 5′-GCGTGCTGTCCCCCTCGGCG-3′.

Multimers (five copies) of the WT or mutated A9 oligonucleotides were made by ligation of *Bgl*II- and *Bam*HI-linked double-stranded oligos and digestion with *Bgl*II and *Bam*HI. For reporter constructs, ligated products were inserted (*Sma*I site) upstream of the TATA box (a 16 bp sequence) from the mouse osteocalcin gene 2 promoter (OG2-TATA box), which is followed by the *Luc* gene. All inserts were confirmed by DNA sequencing.

DNA transfection assay and mutagenesis

COS1 cells were plated at 5×10^4 cells/well in 24-well plates. After 18 hours, the cells were transfected with Lipofectamine. Each transfection contained per well, 0.25 μg of Ihh-Luc, 0.25 μg of Atf4 and 0.025 μg of β-galactosidase (β-gal) plasmids. Luc and β-gal assays were performed 24 hours post-transfection. Data presented are ratios of Luc/β-gal activity from at least three different experiments and each experiment was performed in triplicate for each DNA sample.

Organ culture and purmorphamine treatment

E14 limbs were freed of skin and muscles and cultured in BGJ-B medium with antibiotic/antimycotic (Life Technologies) and 0.5% BSA in a 24-well cell culture plate (Minina et al., 2001) for 4 days at 37°C in 5% CO_2 and humidified atmosphere. Right limbs of each embryo were supplemented with 10 μM purmorphamine (Calbiochem) and left limbs of the same embryo were cultured with DMSO as a control. The experiments were repeated three times. Limb explants were photographed before and after culture and then fixed and embedded in paraffin and sectioned at 5 μm for histological and in situ analyses.

RESULTS

Atf4 is expressed in chondrocytes

To address the function of Atf4 during chondrogenesis, we first analyzed its expression pattern. In whole embryo nuclear extracts, Atf4 protein was detected from embryonic day (E) 9 (9 dpc) to E11. Atf4 was expressed at high levels from E12 to E14 and at low levels from E15 to birth in nuclear extracts of isolated limbs (Fig. 1A). To further confirm that Atf4 was expressed in chondrocytes, nuclear extracts of primary chondrocytes isolated from pup ribs at post-natal day (P) 3 were examined. Atf4 was present at the same level as in primary osteoblasts isolated from P3 pup calvariae. Atf4 was not detected in primary fibroblasts of the same developmental stage (Fig. 1B). These results, together with the fact that Atf4 is not detectable in any other adult tissues except bone (Yang and Karsenty, 2004), eye and cartilage (Fig. 1C), suggest that Atf4 expression is broad in embryos during early development but becomes more restricted to skeletal tissues from E14 onward. Immunohistochemistry revealed that Atf4 was present in all growth plate chondrocytes, with high levels of expression in perichondrium, proliferative and prehypertrophic chondrocytes (Fig. 1D and see Fig. S1A in the supplementary material). Therefore, the expression pattern of Atf4 is consistent with a role in the regulation of chondrocyte biology.

Dwarfism in *Atf4*$^{-/-}$ mice

In analyzing *Atf4*$^{-/-}$ mouse phenotypes we noticed a striking reduction in body size compared with their wild-type (WT) littermates (Fig. 2A). Quantification revealed a 50% reduction in body weight (9.53±1.55 g versus 20.25±1.33 g, P=0.014 by paired Student's t-test, n=4) and in femoral bone length (5.66±0.23 mm versus 10.55±0.08 mm, $P=3\times10^{-7}$, n=7) in 1-month-old mice (Fig. 2B,C), indicating severe limb dwarfism. To determine the onset of this phenotype, we examined embryos stained with Alizarin Red and Alcian Blue and measured their sizes from E9 to E18. The gross sizes of WT and *Atf4*$^{-/-}$ embryos were indistinguishable from E9 to E11 (data not shown), indicating that deletion of *Atf4* did not cause a general reduction in body size prior to the developmental stages during which the first bone elements are shaped. However, *Atf4*$^{-/-}$ embryos appeared smaller than WT littermates at E12, an early stage of chondrogenesis (Fig. 2D), and the small stature was persistent with an increasing penetrance from 55.6% at E12 and 85.6% at E14 to 100% at E16 and birth (Table 1).

Given the severe decrease in limb length at adulthood (Fig. 2C), we focused our analysis on the long bones. At E12, the initial cartilaginous primordia of *Atf4*$^{-/-}$ humeri (black double-headed arrows in Fig. 2D) were smaller compared with WT littermates (red double-headed arrows in Fig. 2D), although the difference was not

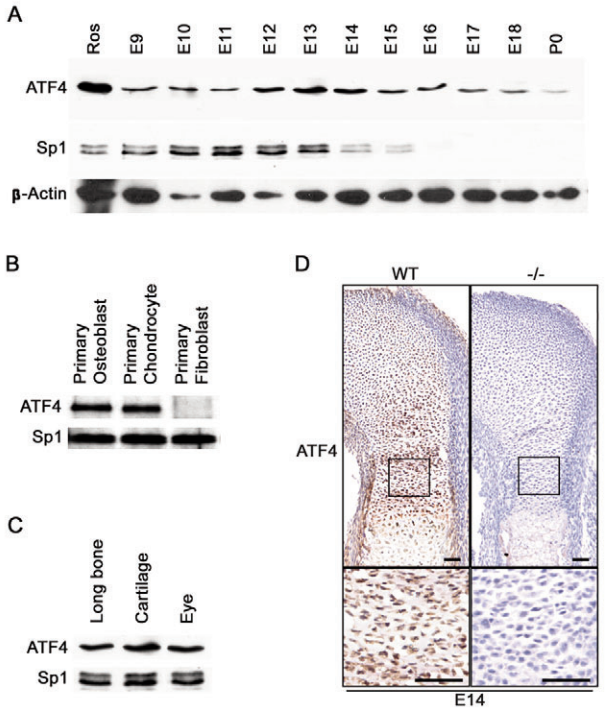

Fig. 1. Atf4 is expressed in chondrocytes. (**A**) Western blot of nuclear extracts of mouse embryos (E9-11) and limbs (E12-P0) for Atf4. Sp1 and β-actin were used as a loading control. (**B**) Western blot of nuclear extracts from the indicated primary cells. (**C**) Western blot of nuclear extracts from the indicated tissues. (**D**) Immunohistochemistry of growth plate sections of E14 wild-type (WT) and mutant (*Atf4*$^{-/-}$) humeri. The boxed regions are magnified beneath. Scale bars: 50 μm.

Table 1. Penetrance of *Atf4*$^{-/-}$ dwarfism

	Developmental stage (dpc)				
Atf4 genotype	12	14	16	Newborn	Total (%)
+/+	17	7	10	14	48 (25.8)
+/–	30	27	10	34	101 (54.3)
–/–	9	7	9	12	37 (19.9)
Dwarfism in –/–	5	6	9	12	
Penetrance (%)	55.6	85.7	100	100	

The number of embryos/pups assayed at each developmental stage is indicated, together with the number of *Atf4*$^{-/-}$ that show dwarfism.

Table 2. Affect of *Atf4* mutation on total and non-mineralized cartilage lengths of humerus

		Length (mm)		
Stage	n	WT	*Atf4*$^{-/-}$	P-value
Total humerus				
E12	4	0.645±0.006	0.620±0.015	0.095
E13	4	0.743±0.011	0.688±0.023	0.050*
E14	4	1.765±0.054	1.463±0.041	0.023*
E16	5	3.186±0.078	2.664±0.059	0.000079**
P0	5	4.164±0.092	3.744±0.052	0.002**
Non-mineralized humerus				
E14	4	1.307±0.030	1.142±0.048	0.013*
E16	5	1.756±0.061	1.629±0.058	0.012**
P0	5	1.515±0.035	1.424±0.042	0.003**

Length is shown as mean ± s.e.
P-value by Student's t-test. *Significant; **strongly significant.

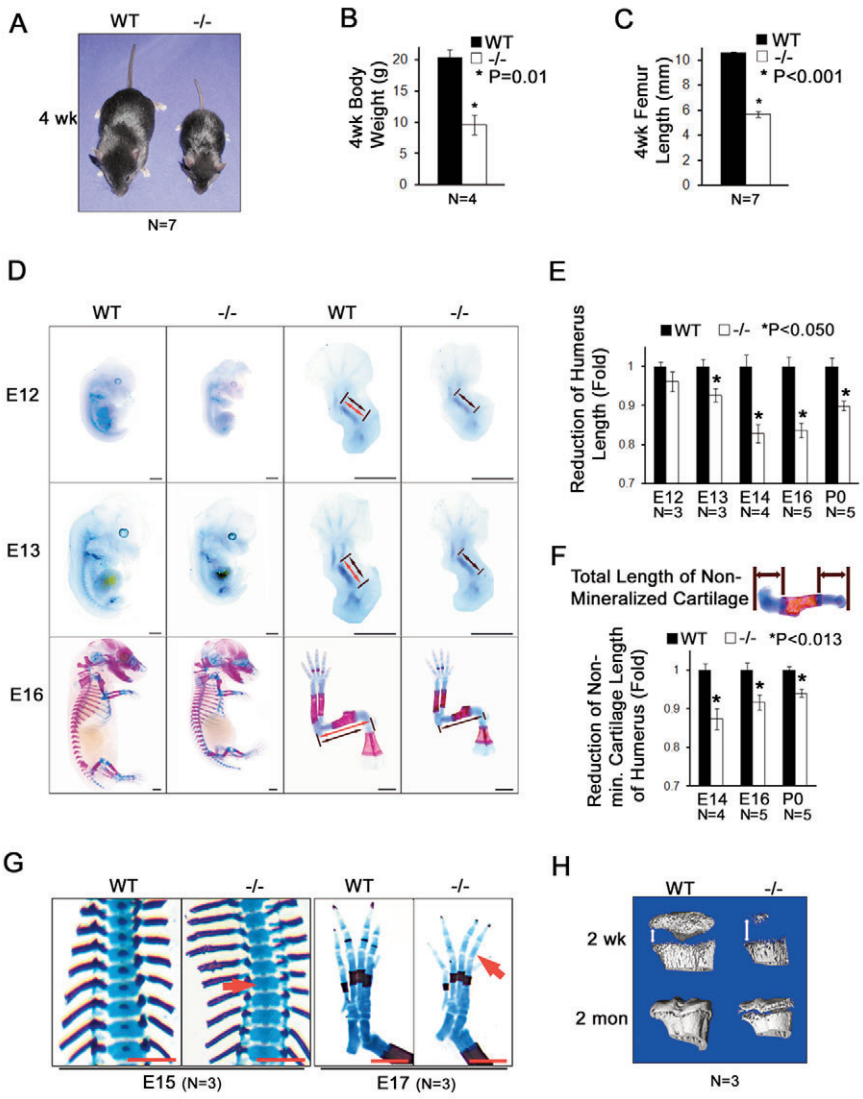

Fig. 2. *Atf4*$^{-/-}$ embryos and mice exhibit dwarfism. (**A**) One-month-old WT and *Atf4*$^{-/-}$ mice. (**B**) Quantification of body weight of 1-month-old WT and *Atf4*$^{-/-}$ mice. Error bars indicate s.e.m.; *n*=4 mice of each genotype. *P*=0.01 by paired Student's *t*-test. (**C**) Quantification of femur length of 1-month-old WT and *Atf4*$^{-/-}$ mice. (**D**) Alizarin Red S and Alcian Blue stained skeletons of embryos and limbs at E12 (12 dpc), E13 and E16. Red and black double-headed arrows represent the length of WT and *Atf4*$^{-/-}$ humeri, respectively. (**E**) Quantification of humerus length during development for WT and *Atf4*$^{-/-}$ mice. Error bars indicate s.e.m. of *Atf4*$^{-/-}$ humerus length normalized to WT humerus length. (**F**) Quantification of non-mineralized cartilage length (top panel, double-headed arrows) in WT and *Atf4*$^{-/-}$ humerus during development. Error bars indicate s.e.m. of *Atf4*$^{-/-}$ normalized to WT humerus non-hypertrophic zone length. (**G**) Alizarin Red S and Alcian Blue stained skeletons of embryos showing a delay in the formation of the primary ossification center in E15 *Atf4*$^{-/-}$ thoracic vertebrae (left, arrow) and E17 hindlimb digits (right, arrow). (**H**) Microtomographic image showing a delay in formation of the secondary ossification center in *Atf4*$^{-/-}$ mice (as indicated by the double-headed arrow). Scale bars: 1 mm.

statistically significant (Table 2). From E13 to birth, the length of *Atf4*$^{-/-}$ humeri decreased by 7% at E13, 17% at E14, 16% at E16 and 10% at birth; this decrease was small but reproducible (Fig. 2D,E and Table 2). To assess the contribution of abnormal *Atf4*$^{-/-}$ chondrocyte function to the short limb phenotype, the length of non-mineralized cartilage in the humerus was measured. A small but significant decrease of 13% at E14, 7% at E16 and 6% at birth was found (Fig. 2F and Table 2). Together, these results suggest that Atf4 is required for chondrocyte function during skeletal development, but that the early condensation of mesenchymal cells to form the anlagen of the future bones and their differentiation into chondrocytes are independent of Atf4.

Delayed hypertrophic mineralization in *Atf4*$^{-/-}$ growth plates

Upon further detailed analysis of skeletal preparations, we found that the mineralization of chondrocytes was also affected by *Atf4* ablation. The first signs of mineralization, which appeared as a single focus of Alizarin Red staining in the center of cartilaginous elements, were detected at E14 in every skeletal element of WT hindlimbs, except for digit bones. However, this staining was only detected in the femur and tibia, but not ilium and fibula, of *Atf4*$^{-/-}$ embryos at this stage (data not shown). Extensive mineralization was detected in all long bones by E15 in WT embryos. However, at this stage, and even at E16 and E17, mineralization in *Atf4*$^{-/-}$ embryos remained absent in some vertebrae (Fig. 2G) and digits (Fig. 2G and see Fig. S1B in the supplementary material). In the post-natal growth plate, 3D-computed microtomographic analysis revealed the presence of a larger gap formed by non-mineralized chondrocyte matrix in *Atf4*$^{-/-}$ tibiae, as compared with WT littermates, at 2 weeks and 2 months of age (Fig. 2H). Together, these results demonstrate that deletion of *Atf4* causes a general delay in growth plate development and subsequent ossification. Therefore, Atf4 is indispensable for chondrocyte hypertrophic mineralization during endochondral ossification.

Proliferative chondrocyte disorganization and delayed hypertrophy in *Atf4*$^{-/-}$ growth plates

To further understand the cause of the *Atf4*$^{-/-}$ mutant phenotypes, we performed histological analyses on developing long bones of the forelimb. At E14, the hypertrophic zone in the center of the WT humerus shaft contained enlarged cells, which were surrounded by invading vasculature and a newly formed cortical bone collar in the perichondrium. The hypertrophic zone in *Atf4*$^{-/-}$ humeri was

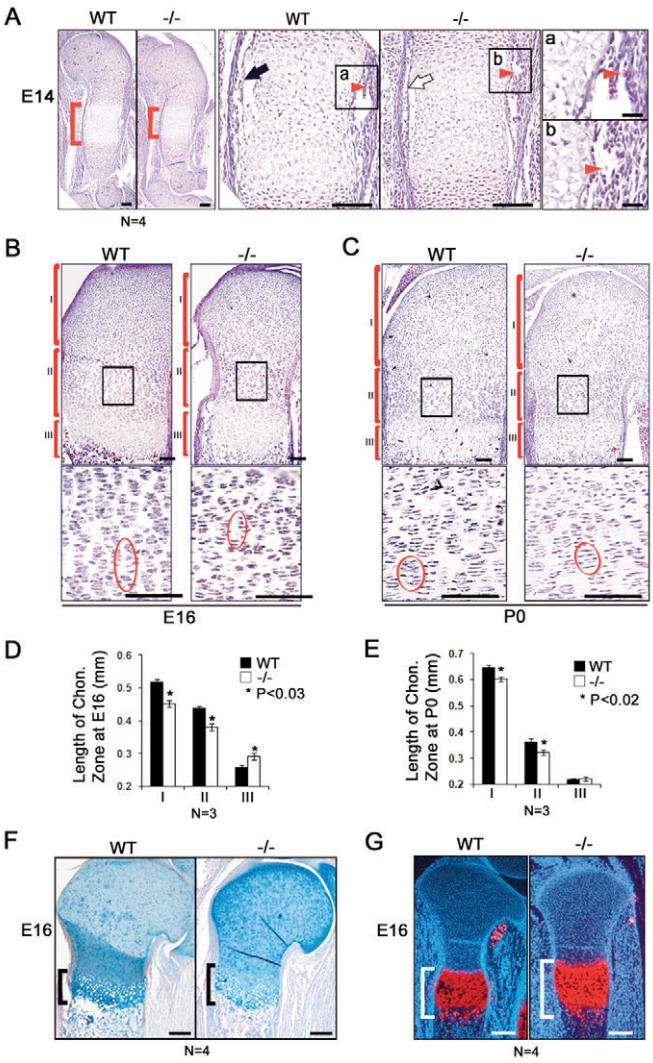

Fig. 3. Decreased proliferation zone and expanded hypertrophic zone of *Atf4*$^{-/-}$ growth plate chondrocytes. (**A**) Hematoxylin and Eosin (H&E) staining of sections through E14 WT and *Atf4*$^{-/-}$ mouse humerus. The center of the humeri (red brackets) are magnified in the middle pair of panels. The black arrow indicates newly formed cortical bone in the WT humerus, which is much thinner in the *Atf4*$^{-/-}$ humerus (white arrow). (**a**,**b**) Higher magnification of the boxed regions of the humerus center showing vascular invasion (arrowheads) in WT and *Atf4*$^{-/-}$ humeri. (**B**,**C**) H&E staining of E16 and P0 WT and *Atf4*$^{-/-}$ humerus sections. Reserve (I), proliferative (II) and hypertrophic (III) chondrocyte zones are indicated. Boxed regions showing proliferating chondrocytes are magnified beneath. The pattern of well-aligned columnar chondrocytes in the E16 WT proliferating zone is completely disorganized in the *Atf4*$^{-/-}$ growth plate (circled). (**D**,**E**) Quantification of the length of the different chondrocyte zones. Error bars indicate s.e.m. In E, P=0.1 for III. Statistical analysis was performed by paired Student's t-test. (**F**) Alizarin Red and Alcian Blue staining of growth plates of the radius showing that the hypertrophic zone (bracket) in *Atf4*$^{-/-}$ growth plates is expanded compared with its WT littermates at E16. (**G**) In situ hybridization showing that the zone of *Col10a1*-expressing chondrocytes (red) is increased compared with WT control. Scale bars: 0.1 mm in A; 0.02 mm in Aa,b; 0.2 mm in F,G.

shorter (Fig. 3A, brackets), suggesting a delay in hypertrophy. In the *Atf4*$^{-/-}$ perichondrium, the cortical bone collar started to form (Fig. 3A, black arrows) and vascular invasion occurred (Fig. 3Aa,b, arrowheads), despite the reduction in the number of enlarged hypertrophic chondrocytes. These data demonstrate that Atf4 is not required for the onset of angiogenesis that initiates osteogenesis and bone collar formation, which is consistent with our previous observations (Yang et al., 2004). Furthermore, at E16, compared with the columnar pattern formed by the long and organized stacks of actively proliferating chondrocytes in the WT, the stacks were short and disorganized in *Atf4*$^{-/-}$ growth plates (Fig. 3B, bottom panels). At birth, columnar chondrocyte stacks were visible but remained disorganized in *Atf4*$^{-/-}$ growth plates (Fig. 3C, bottom panels). The length of the reserve zones was reduced by 13.5% at E16 and 8.3% at birth in *Atf4*$^{-/-}$ growth plates, and the length of the proliferative zones was decreased by 12% at E16 and 11% at birth compared with WT controls (Fig. 3D,E). Unexpectedly, despite the overall shortening and the delay in appearance of hypertrophic mineralization in the growth plate of developing *Atf4*$^{-/-}$ long bones, the length of the hypertrophic zone was increased by 12% at E16 and remained slightly extended at birth (Fig. 3B-F), which was confirmed by expanded zones of *Col10a1*-expressing chondrocytes (Fig. 3G). Collectively, these results demonstrate that Atf4 is required to induce timely hypertrophy at an early stage (i.e. E14), but to inhibit premature hypertrophy at later stages (i.e. E16 and P0) during skeletal development.

Reduced chondrocyte proliferation in *Atf4*$^{-/-}$ long bones

Before hypertrophy, longitudinal cartilage growth relies on fast division of proliferative chondrocytes and slow division of reserve chondrocytes. After hypertrophy and subsequent ossification, longitudinal skeletal growth is dependent on proliferation of both chondrocytes within the growth plate and osteoblasts within the bone (St-Jacques et al., 1999). The decrease in the reserve and proliferative chondrocyte zone length in *Atf4*$^{-/-}$ long bones led us to hypothesize that *Atf4* might be a regulator of chondrocyte proliferation. To address this, we performed in vivo BrdU incorporation assays and found that the chondrocyte proliferative index was significantly decreased in proliferating chondrocytes in *Atf4*$^{-/-}$ E16 embryos and P0 pups (Fig. 4A-C and see Fig. S1C in the supplementary material), in agreement with the observed reduction in proliferative zone size (Figs 2,3). Therefore, Atf4 is required to maintain the high rate of chondrocyte proliferation in the rapidly growing long bones. In addition, in situ TUNEL assay revealed that there was no difference in the number of apoptotic cells between WT and mutant samples from E16 humeri, although there was an increased number of apoptotic hypertrophic chondrocytes in the center of the reserve zone in P0 *Atf4*$^{-/-}$ cartilage (Fig. 4D, green). This result rules out any contribution by delayed apoptosis to the hypertrophic expansion in E16 and P0 *Atf4*$^{-/-}$ growth plates.

Atf4 is required for *Ihh* expression in chondrocytes

To understand the molecular mechanisms that mediate Atf4 function, and particularly to identify potential Atf4 targets, we performed in situ hybridization using chondrocyte markers. At E14, *Ihh* was expressed in prehypertrophic chondrocytes and its expression level increased at E16 and P0 in WT humeri (Fig. 5Aa-c). At E16, a low level of *Ihh* expression was found in osteoblasts in the center of WT long bones. By contrast, *Ihh* expression was not detectable at E14 and barely detectable at E16 in *Atf4*$^{-/-}$ humeri. Although detectable in *Atf4*$^{-/-}$ humeri at P0, the *Ihh* expression level

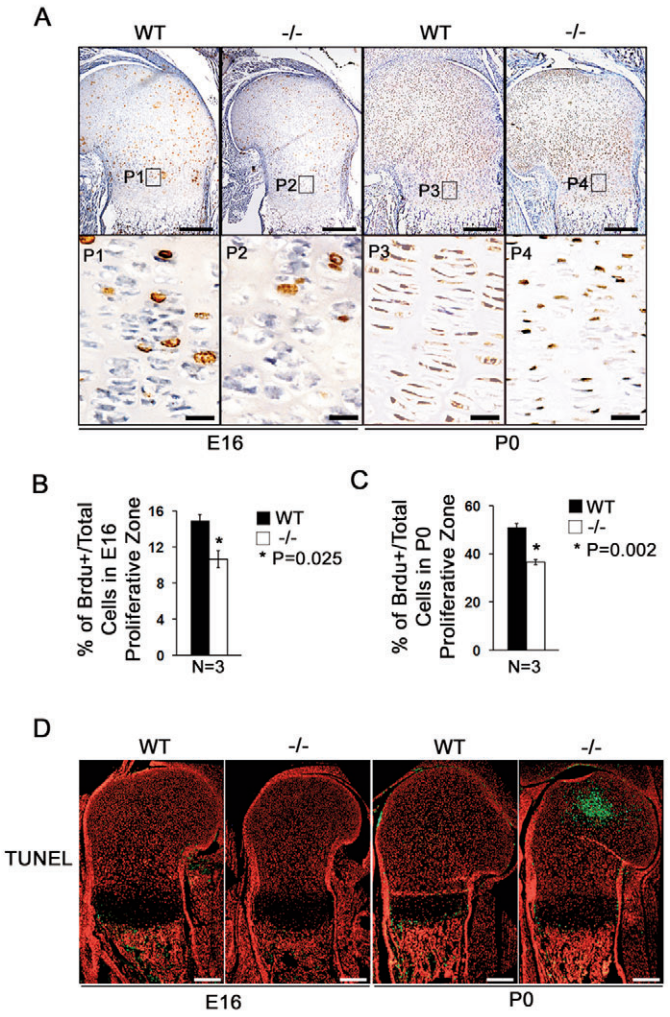

Fig. 4. *Atf4* is required for chondrocyte proliferation. (**A**) BrdU immunohistochemistry of E16 and P0 WT and *Atf4*$^{-/-}$ mouse humerus sections. Boxed regions (P1-P4) are magnified beneath, showing that there are fewer BrdU-positive (brown) proliferative chondrocytes in *Atf4*$^{-/-}$ growth plates in E16 embryos and P0 pups. (**B**,**C**) Quantification of proliferation rate in proliferating chondrocytes, represented by the ratio of BrdU-positive cells normalized to total cells in WT and *Atf4*$^{-/-}$ E16 (B) and P0 (C) humeri. Error bars indicate s.e.m. (**D**) TUNEL assay. In E16 WT and *Atf4*$^{-/-}$ humerus, no apoptotic cells are present in the cartilage, but some TUNEL-positive cells (green) appear in the primary spongiosa. At P0, there are abundant apoptotic cells in the secondary ossification center of the *Atf4*$^{-/-}$ humerus, but not in the WT. There are also some TUNEL-positive cells in primary spongiosa and hypertrophic chondrocyte zones in both WT and *Atf4*$^{-/-}$ growth plate. *n*=5. Scale bars: 0.2 mm in A,D; 0.02 mm in P1-P4 of A.

was substantially lower than that in WT counterparts (Fig. 5Aa′-c′). These results indicate that *Atf4* deletion leads to a delay in the onset of, and a decrease in, *Ihh* expression.

Consistently, the expression of transcription factor *Gli1*, a target and effector of Hh signaling, was decreased in perichondrium and proliferative chondrocytes in *Atf4*$^{-/-}$ humeri at all stages examined (Fig. 5Ad-f′). In E14 WT and *Atf4*$^{-/-}$ humeri, similar expression levels of PTH/PTHrP receptor (*PPR*; *Pth1r* – Mouse Genome Informatics) were detected in prehypertrophic chondrocytes, the same domain in which *Ihh* was expressed (Fig. 5Ag,g′). Interestingly, *PPR* expression transiently expanded to cells of the periosteum and to osteoblasts at E16, yet diminished in osteoblasts at birth in both WT and *Atf4*$^{-/-}$ humeri (Fig. 5Ah-i′).

There was no difference in *Col2a1* expression between WT and *Atf4*$^{-/-}$ humeri, although the zone of *Col2a1*-expressing chondrocytes was shorter in *Atf4*$^{-/-}$ bones (Fig. 5Aj-l′). At E14 in WT humeri, *Col10a1*-expressing hypertrophic chondrocytes had already separated into two distinct zones, whereas they appeared to be one single mass at the center in *Atf4*$^{-/-}$ humeri (Fig. 5Am,m′). There were no differences in the *Col10a1* expression level between WT and mutant humeri at any of the stages examined (Fig. 5Am-o′). However, at E16, mutant *Col10a1*-expressing hypertrophic chondrocyte zones were slightly expanded compared with their WT counterparts (Fig. 5An,n′). At birth, *Col10a1*-expressing hypertrophic chondrocyte zones remained unchanged, or were expanded, if one takes into account the overall length of the humeri (Fig. 5Al,l′). The pattern of *Col10a1* expression was consistent with the delay in long-bone mineralization and with the transient expansion of the hypertrophic zone at E16 (Figs 2,3).

Since the level of *Ihh* transcripts, as well as that of its downstream target gene *Gli1*, appeared to be reduced in the absence of *Atf4*, as judged by in situ hybridization, we further quantified the expression of these genes. qRT-PCR results confirmed a 60% decrease in *Ihh* expression in E14 *Atf4*$^{-/-}$ cartilage. Consistently, we observed a decrease in the expression of *PTHrP* (45%) and *Gli1* (41%), two downstream targets of the Hh signaling (Fig. 5B). Furthermore, and consistent with the in situ hybridization results, the expression of *PPR* was normal in E14 *Atf4*$^{-/-}$ cartilage. Taken together, these data strongly suggest that Atf4 is specifically required for *Ihh* expression in chondrocytes in vivo and that the decrease in *Ihh* expression is not a generalized consequence of *Atf4* deficiency.

Atf4 directly regulates *Ihh* transcription

To test whether *Ihh* is a direct transcriptional target of Atf4, we examined whether overexpression of Atf4 could affect endogenous *Ihh* mRNA levels in TMC23 chondrocytes (Xu et al., 1998). Atf4 overexpression induced endogenous *Ihh* expression to an extent similar to that induced by Runx2 overexpression (Fig. 6A). To address whether this function of Atf4 was direct, we co-transfected Ihh reporter constructs (pIhh-1.3-Luc and pIhh-742-Luc) individually with an Atf4 expression plasmid into COS1 cells. Both reporter constructs were transactivated by Atf4 to a similar extent (Fig. 6B), suggesting that the 742 bp promoter fragment of *Ihh* might contain an Atf4 binding site(s).

We examined the 742 bp promoter fragment of *Ihh* and located nine putative Atf4 binding sites, named A1 to A9 (Fig. 6C). EMSA revealed that Atf4 bound strongly to A9, but not to the other eight probes (Fig. 6D). Consistently, Atf4 failed to transactivate luciferase activity on pIhh-715-Luc, a construct in which A9 is deleted (Fig. 6B). Furthermore, Atf4 transactivated a reporter containing five repeats of A9 (pII5xA9-Luc) more than 5-fold (Fig. 6E), yet did not activate a reporter containing five copies of a mutant A9 sequence (PII5xmA9-Luc) that binds Atf4 with ten times lower affinity (Fig. 6F,G).

EMSA revealed that endogenous Atf4 from WT, but not *Atf4*$^{-/-}$, primary chondrocytes bound to A9 (Fig. 6H). In addition, Atf4 antibody inhibited protein-A9 complex formation, whereas an unrelated control antibody had no effect (Fig. 6I). Taken together, these results confirm that the A9 sequence of the *Ihh* promoter serves as an Atf4 binding site, mediating Atf4 transactivation of *Ihh* transcription.

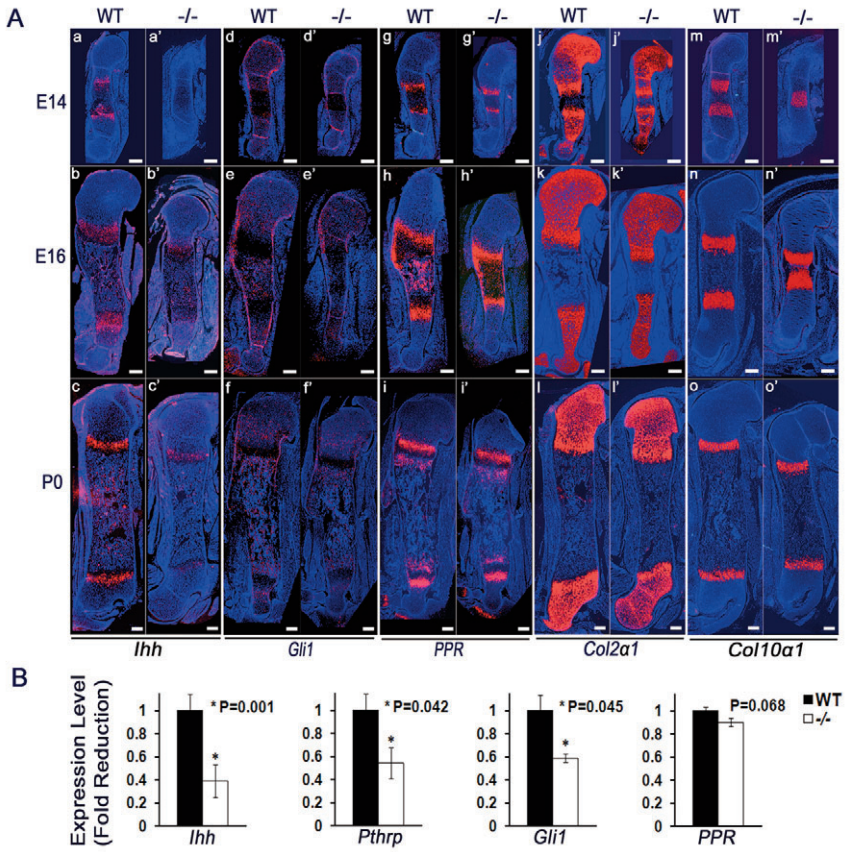

Fig. 5. *Ihh* expression is decreased in *Atf4*$^{-/-}$ cartilage. (**Aa-o'**) In situ hybridization of sections of E14, E16 and P0 WT and *Atf4*$^{-/-}$ mouse humeri. Note the decrease in *Ihh* and *Gli1*, but normal *PPR* (*Pth1r*), expression in *Atf4*$^{-/-}$ growth plates. Although the *Col2a1*-positive zones are shorter and the *Col10a1*-positive zones are slightly longer than their WT counterparts at every stage examined, the expression of *Col2a1* and *Col10a1* was unchanged in *Atf4*$^{-/-}$ growth plates. Scale bars: 0.2 mm. (**B**) qRT-PCR analysis showing decreased levels of *Ihh*, *PTHrP* (*Pthlh*) and *Gli1* and normal levels of *PPR* mRNA in E14 *Atf4*$^{-/-}$ cartilage. Data are normalized to expression levels in WT cartilage and 18S rRNA (n=3).

An Ihh agonist partially restores the length of *Atf4*$^{-/-}$ limbs

Since *Col2a1-Ihh* transgenic mice were not viable, we designed a rescue experiment based on an organ culture system. Limb explants from WT and *Atf4*$^{-/-}$ E14 embryos were cultured in the presence or absence of purmorphamine, a synthetic compound that directly targets smoothened to activate Hh signaling (Sinha and Chen, 2006). At the beginning of the culture (t0), the primary ossification center was formed in WT ulna, but not in WT radii. As expected, no visible ossification center was present in mutant long bones at this stage (Fig. 7A, arrowheads). After 4 days of growth (t4), ossification centers were observed in both the ulna and radii in both genotypes (Fig. 7A, arrowheads), indicating a normal sequence of limb development in this organ culture system.

Hh signaling reactivation upon purmorphamine treatment was confirmed by increased *Gli1* expression in purmorphamine-treated *Atf4*$^{-/-}$ limbs as compared with vehicle-treated samples (Fig. 7Ah,i). Within 4 days of growth, the length of the radii increased by 31% in WT and by 21% in purmorphamine-treated *Atf4*$^{-/-}$limbs, whereas it increased only 10% in vehicle-treated mutant limbs (Fig. 7B). These results indicate that reactivation of Hh signaling improves the longitudinal growth of *Atf4*$^{-/-}$ limbs in culture. The increase in size in purmorphamine-treated *Atf4*$^{-/-}$ limbs was associated with elongated zones of proliferative and hypertrophic chondrocytes (Fig. 7Ca-c,D). In addition, purmorphamine reduced the delayed hypertrophy in *Atf4*$^{-/-}$ limbs, as shown by the increase in the *Col10a1*-expressing chondrocyte area in purmorphamine-treated versus vehicle-treated *Atf4*$^{-/-}$ radii (Fig. 7Ce,f,D). The BrdU proliferative index in proliferative chondrocytes (Fig. 7E, arrowheads) was significantly increased upon purmorphamine treatment of *Atf4*$^{-/-}$ limbs (Fig. 7F). These results indicate that activation of the Hh pathway in *Atf4*$^{-/-}$ limbs can partially rescue the defects in chondrocyte proliferation and hypertrophy characteristic of this mutant, further reinforcing the notion that Atf4 and Ihh lie in the same pathway for the regulation of limb development and long-bone growth.

DISCUSSION

This study reveals the transcription factor Atf4 as a crucial regulator of chondrogenesis and identifies *Ihh* as a transcriptional target of Atf4 in chondrocytes. Mice lacking Atf4 exhibit dwarfism and are characterized by markedly reduced growth plates, decreased chondrocyte proliferation and an abnormally expanded hypertrophic zone. These phenotypic abnormalities are similar to those of *Ihh*$^{-/-}$ mice (St-Jacques et al., 1999), which, together with the dramatic decrease in *Ihh* expression observed in *Atf4*$^{-/-}$ growth plates, indicate that Atf4 and Ihh lie in the same genetic pathway regulating chondrogenesis during skeletal development.

Distribution of Atf4 in chondrocytes

Atf4 was originally termed osteoblast-specific factor 1 (Osf1) because it was first identified as a specific binding activity of osteoblast nuclear extracts to OSE1, the osteoblast-specific element 1 found in the osteocalcin (*Bglap*) promoter (Ducy and Karsenty, 1995). Subsequent studies revealed that the cell specificity of Atf4 is regulated at the post-translational level (Yang and Karsenty, 2004). However, nuclear extracts of primary chondrocytes were not tested in previous studies, and the evidence for involvement of Atf4 in chondrogenesis was lacking. In this study, a systematic analysis of the expression pattern of Atf4 demonstrated that it is expressed at high levels in embryos, limbs and primary chondrocytes, supporting its role in chondrogenesis.

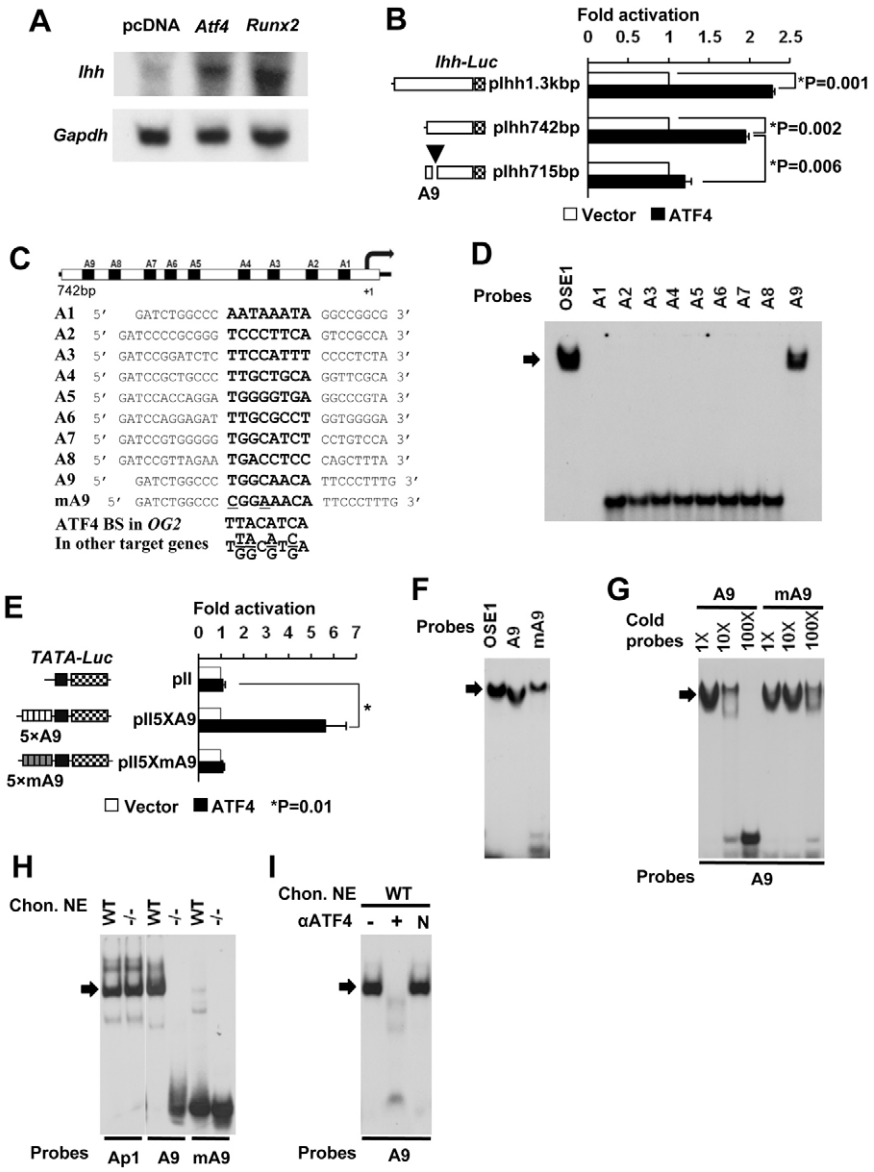

Fig. 6. Atf4 binds to the *Ihh* promoter to activate transcription. (**A**) Northern blot analysis showing that Atf4 and Runx2 stimulate endogenous *Ihh* mRNA expression in TMC23 cells. *Gapdh* serves as a loading control. (**B**) Atf4 activates *Ihh* promoter reporters in COS1 cells. Co-transfection assay showing that Atf4 activates *Ihh* promoter reporters (pIhh-1.3kbp and pIhh-742bp, as shown to left) but not the construct containing a mutated A9 (arrowhead), the Atf4 binding site. (**C**) Sequences of nine putative Atf4 binding sites (A1-A9) in the proximate 742 bp promoter region of the mouse *Ihh* gene. Core sequences are indicated in bold, being identical to those within the Atf4 consensus sequence [i.e. TTACATCA, OSE1 in osteocalcin (*OG2*) and T(T/G)(A/G)C(A/G)T(C/G)A in other Atf4 target genes]. (**D**) Atf4 binds to A9 in the *Ihh* promoter. EMSA using the nine ^{32}P-labeled putative Atf4 binding sites, A1-A9, as probes with purified His-tagged Atf4 recombinant protein. OSE1 serves as a positive control. Arrow, Aft4-probe complex. (**E**) A9 mediates Atf4 transactivation of *Ihh*. p5XA9-Luc and p5XmA9-Luc contain five copies of WT and mutant A9 [which binds Atf4 only weakly (see F,G)], respectively, linked to a TATA-box vector. (**F**) EMSA using ^{32}P-labeled probes at equal counts per minute of OSE1, A9 and A9 mutant (A9mut). Note the large amount of unbound A9mut probe at the bottom of the gel. (**G**) Competition EMSAs. Fold molar excess of unlabeled double-stranded DNA competitor over labeled probe is indicated. (**H**) Endogenous Atf4 binds to A9. The Ap1 probe, the cJun/cFos binding site, was used as a control for nuclear extract quality. (**I**) Supershift EMSAs showing that an antibody against Atf4 inhibits the binding of endogenous Atf4 to A9 (lane +). N, unrelated antibody.

Atf4 as a novel transcriptional regulator of *Ihh*

A major finding of this study is that Atf4 directly regulates chondrocyte proliferation by affecting the transcription of *Ihh*, a molecule that plays crucial roles in both chondrogenesis and osteogenesis. We demonstrated, for the first time genetically and molecularly, that Atf4 acts as a direct transcriptional activator of *Ihh*, the expression of which is dramatically decreased in *Atf4* mutant mice. Atf4 binds and transactivates *Ihh* in chondrocytes and forced expression of Atf4 enhances endogenous *Ihh* mRNA synthesis. In organ cultures, reactivation of Hh signaling by a synthetic compound that bypasses the need for Ihh ligand almost completely rescues the proliferation defects and partially rescues the delay in hypertrophy in *Atf4*$^{-/-}$ limbs. As a result, the short limb phenotype in *Atf4*$^{-/-}$ animals was partially corrected. Together, these results strongly suggest that Atf4 and Ihh act in the same pathway to regulate chondrocyte proliferation and hypertrophy. The fact that the hypertrophic defect in *Atf4*$^{-/-}$ limbs was not fully rescued by purmorphamine might suggest that Atf4 regulates chondrocyte hypertrophy by an additional and Ihh-independent mechanism(s), or, more likely, it might reflect a limitation of the organ culture system.

The functions of Atf4 and Runx2, another transcriptional activator of *Ihh*, are not redundant as removal of *Atf4* or *Runx2* gives rise to severe chondrocyte proliferation or differentiation defects, respectively. Although our current study cannot dissect the relative contributions of Runx2 and Atf4 to the control of chondrogenesis, the fact that *Runx2*$^{-/-}$ animals completely lack hypertrophic chondrocytes in their skeletons (Komori et al., 1997; Otto et al., 1997), and that the role of Runx2 is in the induction, rather than inhibition, of chondrocyte hypertrophy (Takeda et al., 2001; Ueta et al., 2001), suggest that the function of Runx2 in the control of chondrocyte biology could be Ihh-independent and antiproliferative. In fact, a recent study showed that Runx2 inhibits chondrocyte proliferation and hypertrophy through regulation of *Fgf18* transcription in the perichondrium (Hinoi et al., 2006). It is unlikely that Atf4 regulates *Fgf18* directly because overexpressing Atf4 has no effect on luciferase activity driven by *Fgf18* promoter constructs in DNA co-transfection assays (Dr M. Naski, personal communication). Consistently, we observed no differences in the expression of *Fgf18* in WT and *Atf4*$^{-/-}$ cartilage (see Fig. S2A in the supplementary material). Other studies indicate that *Runx2* mRNA

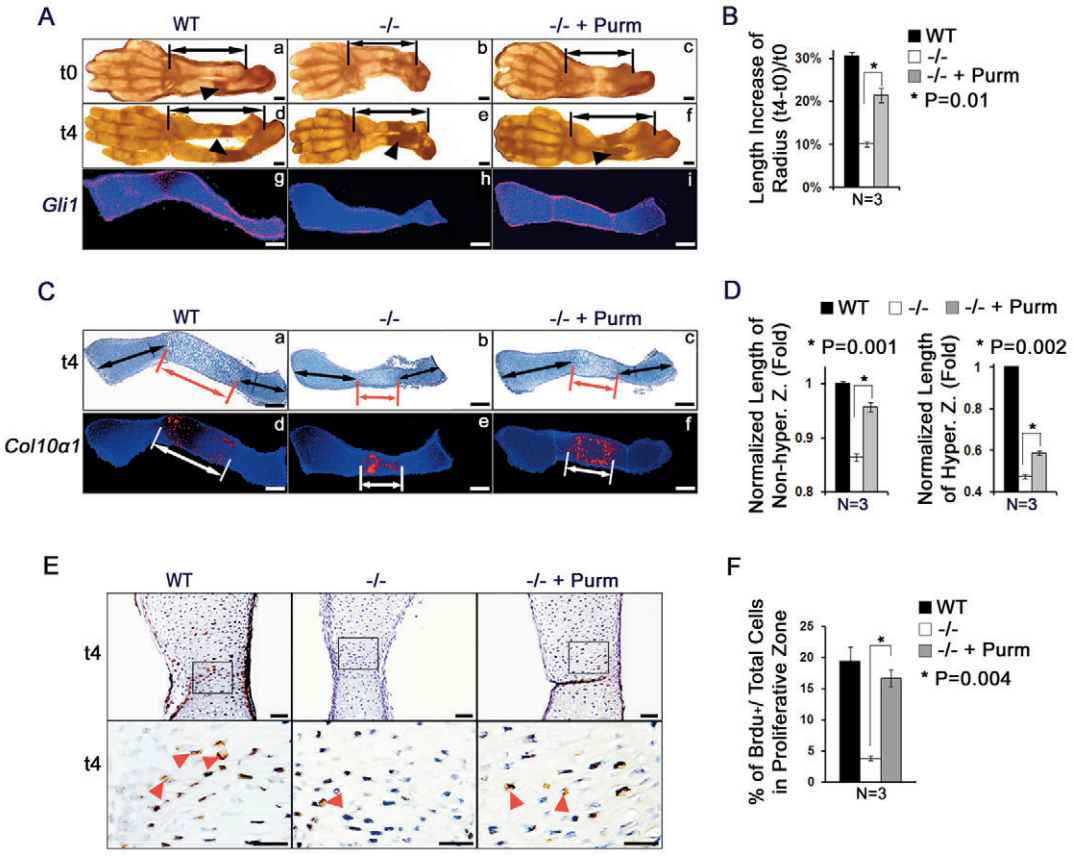

Fig. 7. Reactivation of Hh signaling by purmorphamine rescues limb defects in *Atf4*$^{-/-}$ embryos. (**A**) Purmorphamine, an agonist of the Hh signaling pathway, restores the length of the *Atf4*$^{-/-}$ forelimb in organ cultures. (**a-f**) Limb explants at the beginning (t0, a-c) and the end (4 days, t4, d-f) of culture. *n*=3. Purmorphamine partially rescued the longitudinal growth of the *Atf4*$^{-/-}$ radius (double-headed arrow, f) as compared with the control (e). Arrowheads indicate BrdU-positive cells. (**g-i**) In situ hybridization of *Gli1* expression in WT (g), vehicle-treated *Atf4*$^{-/-}$ (h), and purmorphamine-treated *Atf4*$^{-/-}$ (i) radii. *n*=3. Purmorphamine restored *Gli1* expression in *Atf4*$^{-/-}$ radii (i) to a level similar to that in WT controls (h), indicating activation of Hh signaling in *Atf4*$^{-/-}$ explants. (**B**) Quantification of the increase in radius length upon purmorphamine treatment of WT and *Atf4*$^{-/-}$ limbs. The percentage increase in radius growth after 4 days in culture is shown. *P*=0.01 by paired Student's *t*-test. (**C**) Purmorphamine partially corrects the delayed chondrocyte hypertrophy in *Atf4*$^{-/-}$ growth plates in organ culture. (**a-c**) Alcian Blue, Alizarin Red and Hematoxylin staining of radius sections of 4-day cultures. (**d-f**) In situ hybridization for *Col10a1* in purmorphamine-treated and vehicle-treated limb explants. *n*=3. (**D**) Quantification of the relative length of the non-hypertrophic and hypertrophic zones upon purmorphamine treatment of WT and *Atf4*$^{-/-}$ radii. Error bars indicate s.e.m. of the length of the non-hypertrophic (left) and hypertrophic (right) zones normalized to the respective WT controls at 4 days in culture. (**E**) Purmorphamine increases chondrocyte proliferation in *Atf4*$^{-/-}$ growth plates. Immunohistochemistry of BrdU-labeled chondrocytes in limbs cultured for 4 days in the absence and presence of purmorphamine. The sections were counterstained with Hematoxylin. Boxed regions are magnified beneath to show BrdU-positive cells (arrowheads). *n*=3. (**F**) Quantification of proliferation rate represented by the ratio of BrdU-positive cells (brown) to total cells upon purmorphamine treatment of WT and *Atf4*$^{-/-}$ radii. Error bars indicate s.e.m. Scale bars: 0.2 mm in A,C; 0.5 mm in E.

synthesis can be downregulated by PTH/PTHrP signaling (Guo et al., 2006), yet *Atf4* mRNA and protein are upregulated by parathyroid hormone (Yu et al., 2008), supporting the notion that Atf4 and Runx2 play different, but related, roles in the regulation of chondrogenesis.

Atf4 regulates chondrocyte differentiation

The fact that the hypertrophic chondrocyte zone in *Atf4*$^{-/-}$ long bones is transiently increased at E16 and then remains the same as in WT, and that *PTHrP* expression is downregulated in *Atf4* mutant growth plates, indicate that Atf4 plays a role in the control of hypertrophic chondrocyte differentiation. This provides indirect confirmation that *Ihh* expression is downregulated in *Atf4*$^{-/-}$ growth plates. PTHrP and its receptor, which lie downstream of Ihh signaling, play multiple roles in regulating chondrocyte proliferation and differentiation (Kronenberg, 2006). PTHrP acts as an inhibitor to prevent premature chondrocyte hypertrophy (Karaplis et al., 1994), which ensures the maintenance of a pool of proliferative chondrocytes. PTHrP also directly stimulates chondrocyte proliferation in an organ culture system (Mau et al., 2007). However, it is unclear whether Atf4 is a direct transcriptional regulator of *PTHrP* or not. Our DNA transfection data suggest that the downregulation of *PTHrP* expression in *Atf4*$^{-/-}$ chondrocytes might be due to an indirect mechanism, most likely involving impaired Hh signaling, as: (1) Atf4 did not transactivate luciferase constructs driven by 4.5 or 1.1 kb *PTHrP* promoter fragments, whereas these two reporter constructs responded to Gli2, a known transcriptional activator of *PTHrP* (Sterling et al., 2006; Zhao, 2005) (see Fig. S2B,C in the supplementary material); and (2) we could not locate any Atf4 binding consensus site within this promoter region.

Type II collagen secretion is normal in *Atf4*$^{-/-}$ chondrocytes

Given the indispensable role of Atf4 in the regulation of stress responses (Harding et al., 2000; Harding et al., 2003; Rutkowski and Kaufman, 2003) and in type I collagen synthesis in osteoblasts (Yang et al., 2004), Atf4 may be required for secretion of type II collagen in chondrocytes. Our immunohistochemistry results using a monoclonal antibody developed by Dr Thomas F. Linsenmayer (Tufts Medical School, Boston, MA, USA) revealed that type II collagen secretion is normal in *Atf4*$^{-/-}$ cartilage (see Fig. S2C in the supplementary material). Furthermore, we also observed a normal expression level of hypoxia-inducible factor 1 (see Fig. S2E in the supplementary material), a master regulator of oxygen homeostasis and a key element to cellular survival and adaptation and a regulator of chondrogenesis (Amarilio et al., 2007). These results cannot rule out the possibility that Atf4 plays a role in the response to oxygen level in chondrocytes, given the hypoxic environment in which chondrocytes exist.

This study reveals a novel mechanism by which Atf4 regulates chondrocyte proliferation and differentiation via upregulating *Ihh* expression. It remains unclear, however, what upstream signals regulate Atf4 expression and activity and what downstream effector molecules of Hh signaling are controlling chondrocyte proliferation and differentiation. Many extracellular regulators, including members of the FGF, BMP, Igf1, Wnt and PTHrP families, are reported to regulate chondrocyte proliferation and differentiation. Whether they act on chondrocytes by modifying Atf4 activity remains to be determined. Lastly, and importantly, it is of interest to establish whether the same mechanisms are responsible for the bone defects seen in the *Atf4*$^{-/-}$ mice.

Acknowledgements

We thank Drs C. Chiang, M. Patel and T. Schinke for critical comments on the manuscript and Drs G. Mundy, M. Naski and J. Sterling for sharing unpublished data. The monoclonal anti-Col II antibody developed by Dr Thomas F. Linsenmayer was obtained from the Developmental Studies Hybridoma Bank developed under the auspices of the NICHD and maintained by The University of Iowa, Department of Biological Science, Iowa, IA 52242, USA. This work was funded by grants from the March of Dimes Foundation (to X.Y.) and National Institute of Arthritis and Musculoskeletal and Skin Diseases (to X.Y. and E.F.). Deposited in PMC for release after 12 months.

Competing interests statement

The authors declare no competing commercial interests.

Supplementary material

Supplementary material for this article is available at http://dev.biologists.org/cgi/content/full/136/24/4143/DC1

References

Albrecht, J. H., Poon, R. Y., Ahonen, C. L., Rieland, B. M., Deng, C. and Crary, G. S. (1998). Involvement of p21 and p27 in the regulation of CDK activity and cell cycle progression in the regenerating liver. *Oncogene* **16**, 2141-2150.

Alcedo, J. and Noll, M. (1997). Hedgehog and its patched-smoothened receptor complex: a novel signalling mechanism at the cell surface. *Biol. Chem.* **378**, 583-590.

Amano, K., Ichida, F., Sugita, A., Hata, K., Wada, M., Takigawa, Y., Nakanishi, M., Kogo, M., Nishimura, R. and Yoneda, T. (2008). MSX2 stimulates chondrocyte maturation by controlling Ihh expression. *J. Biol. Chem.* **283**, 29513-29521.

Amarilio, R., Viukov, S. V., Sharir, A., Eshkar-Oren, I., Johnson, R. S. and Zelzer, E. (2007). HIF1alpha regulation of Sox9 is necessary to maintain differentiation of hypoxic prechondrogenic cells during early skeletogenesis. *Development* **134**, 3917-3928.

Chung, U. I., Schipani, E., McMahon, A. P. and Kronenberg, H. M. (2001). Indian hedgehog couples chondrogenesis to osteogenesis in endochondral bone development. *J. Clin. Invest.* **107**, 295-304.

Day, T. F. and Yang, Y. (2008). Wnt and hedgehog signaling pathways in bone development. *J. Bone Joint Surg. Am.* **90 Suppl. 1**, 19-24.

de Crombrugghe, B., Vuorio, T., Karsenty, G., Maity, S., Rutheshouser, E. C. and Goldberg, H. (1991). Transcriptional control mechanisms for the expression of type I collagen genes. *Ann. Rheum. Dis.* **50 Suppl. 4**, 872-876.

Ducy, P. and Karsenty, G. (1995). Two distinct osteoblast-specific cis-acting elements control expression of a mouse osteocalcin gene. *Mol. Cell. Biol.* **15**, 1858-1869.

Ducy, P., Zhang, R., Geoffroy, V., Ridall, A. L. and Karsenty, G. (1997). Osf2/Cbfa1: a transcriptional activator of osteoblast differentiation. *Cell* **89**, 747-754.

Guo, J., Chung, U. I., Yang, D., Karsenty, G., Bringhurst, F. R. and Kronenberg, H. M. (2006). PTH/PTHrP receptor delays chondrocyte hypertrophy via both Runx2-dependent and -independent pathways. *Dev. Biol.* **292**, 116-128.

Harding, H. P., Novoa, I., Zhang, Y., Zeng, H., Wek, R., Schapira, M. and Ron, D. (2000). Regulated translation initiation controls stress-induced gene expression in mammalian cells. *Mol. Cell* **6**, 1099-1108.

Harding, H. P., Zhang, Y., Zeng, H., Novoa, I., Lu, P. D., Calfon, M., Sadri, N., Yun, C., Popko, B., Paules, R. et al. (2003). An integrated stress response regulates amino acid metabolism and resistance to oxidative stress. *Mol. Cell* **11**, 619-633.

Hinoi, E., Bialek, P., Chen, Y. T., Rached, M. T., Groner, Y., Behringer, R. R., Ornitz, D. M. and Karsenty, G. (2006). Runx2 inhibits chondrocyte proliferation and hypertrophy through its expression in the perichondrium. *Genes Dev.* **20**, 2937-2942.

Karaplis, A. C., Luz, A., Glowacki, J., Bronson, R. T., Tybulewicz, V. L., Kronenberg, H. M. and Mulligan, R. C. (1994). Lethal skeletal dysplasia from targeted disruption of the parathyroid hormone-related peptide gene. *Genes Dev.* **8**, 277-289.

Karp, S. J., Schipani, E., St-Jacques, B., Hunzelman, J., Kronenberg, H. and McMahon, A. P. (2000). Indian hedgehog coordinates endochondral bone growth and morphogenesis via parathyroid hormone related-protein-dependent and -independent pathways. *Development* **127**, 543-548.

Karsenty, G. (2001). Transcriptional control of osteoblast differentiation. *Endocrinology* **142**, 2731-2733.

Karsenty, G. and Wagner, E. F. (2002). Reaching a genetic and molecular understanding of skeletal development. *Dev. Cell* **2**, 389-406.

Kaufman, M. H. (1992). *The Atlas of Mouse Development*. London: Academic Press.

Komori, T., Yagi, H., Nomura, S., Yamaguchi, A., Sasaki, K., Deguchi, K., Shimizu, Y., Bronson, R. T., Gao, Y. H., Inada, M. et al. (1997). Targeted disruption of Cbfa1 results in a complete lack of bone formation owing to maturational arrest of osteoblasts. *Cell* **89**, 755-764.

Kronenberg, H. M. (2003). Developmental regulation of the growth plate. *Nature* **423**, 332-336.

Kronenberg, H. M. (2006). PTHrP and skeletal development. *Ann. N. Y. Acad. Sci.* **1068**, 1-13.

Mackie, E. J., Ahmed, Y. A., Tatarczuch, L., Chen, K. S. and Mirams, M. (2008). Endochondral ossification: how cartilage is converted into bone in the developing skeleton. *Int. J. Biochem. Cell Biol.* **40**, 46-62.

Mak, K. K., Kronenberg, H. M., Chuang, P. T., Mackem, S. and Yang, Y. (2008). Indian hedgehog signals independently of PTHrP to promote chondrocyte hypertrophy. *Development* **135**, 1947-1956.

Masuoka, H. C. and Townes, T. M. (2002). Targeted disruption of the activating transcription factor 4 gene results in severe fetal anemia in mice. *Blood* **99**, 736-745.

Mau, E., Whetstone, H., Yu, C., Hopyan, S., Wunder, J. S. and Alman, B. A. (2007). PTHrP regulates growth plate chondrocyte differentiation and proliferation in a Gli3 dependent manner utilizing hedgehog ligand dependent and independent mechanisms. *Dev. Biol.* **305**, 28-39.

Minina, E., Wenzel, H. M., Kreschel, C., Karp, S., Gaffield, W., McMahon, A. P. and Vortkamp, A. (2001). BMP and Ihh/PTHrP signaling interact to coordinate chondrocyte proliferation and differentiation. *Development* **128**, 4523-4534.

Nilsson, O., Marino, R., De Luca, F., Phillip, M. and Baron, J. (2005). Endocrine regulation of the growth plate. *Horm. Res.* **64**, 157-165.

Ornitz, D. M. (2005). FGF signaling in the developing endochondral skeleton. *Cytokine Growth Factor Rev.* **16**, 205-213.

Otto, F., Thornell, A. P., Crompton, T., Denzel, A., Gilmour, K. C., Rosewell, I. R., Stamp, G. W., Beddington, R. S., Mundlos, S., Olsen, B. R. et al. (1997). Cbfa1, a candidate gene for cleidocranial dysplasia syndrome, is essential for osteoblast differentiation and bone development. *Cell* **89**, 765-771.

Rutkowski, D. T. and Kaufman, R. J. (2003). All roads lead to ATF4. *Dev. Cell* **4**, 442-444.

Schinke, T. and Karsenty, G. (1999). Characterization of Osf1, an osteoblast-specific transcription factor binding to a critical cis-acting element in the mouse osteocalcin promoters. *J. Biol. Chem.* **274**, 30182-30189.

Shaywitz, A. J. and Greenberg, M. E. (1999). CREB: a stimulus-induced transcription factor activated by a diverse array of extracellular signals. *Annu. Rev. Biochem.* **68**, 821-861.

Sinha, S. and Chen, J. K. (2006). Purmorphamine activates the Hedgehog pathway by targeting Smoothened. *Nat. Chem. Biol.* **2**, 29-30.
St-Jacques, B., Hammerschmidt, M. and McMahon, A. P. (1999). Indian hedgehog signaling regulates proliferation and differentiation of chondrocytes and is essential for bone formation. *Genes Dev.* **13**, 2072-2086.
Sterling, J. A., Oyajobi, B. O., Grubbs, B., Padalecki, S. S., Munoz, S. A., Gupta, A., Story, B., Zhao, M. and Mundy, G. R. (2006). The hedgehog signaling molecule Gli2 induces parathyroid hormone-related peptide expression and osteolysis in metastatic human breast cancer cells. *Cancer Res.* **66**, 7548-7553.
Takeda, S., Bonnamy, J. P., Owen, M. J., Ducy, P. and Karsenty, G. (2001). Continuous expression of Cbfa1 in nonhypertrophic chondrocytes uncovers its ability to induce hypertrophic chondrocyte differentiation and partially rescues Cbfa1-deficient mice. *Genes Dev.* **15**, 467-481.
Ueta, C., Iwamoto, M., Kanatani, N., Yoshida, C., Liu, Y., Enomoto-Iwamoto, M., Ohmori, T., Enomoto, H., Nakata, K., Takada, K. et al. (2001). Skeletal malformations caused by overexpression of Cbfa1 or its dominant negative form in chondrocytes. *J. Cell Biol.* **153**, 87-100.
Xu, C., Ji, X., Harris, M. A., Mundy, G. R. and Harris, S. E. (1998). A clonal chondrocytic cell line derived from BMP-2/T antigen-expressing transgenic mouse. *In Vitro Cell Dev. Biol. Anim.* **34**, 359-363.
Yang, X. and Karsenty, G. (2004). ATF4, the osteoblast accumulation of which is determined post-translationally, can induce osteoblast-specific gene expression in non-osteoblastic cells. *J. Biol. Chem.* **279**, 47109-47114.
Yang, X., Matsuda, K., Bialek, P., Jacquot, S., Masuoka, H. C., Schinke, T., Li, L., Brancorsini, S., Sassone-Corsi, P., Townes, T. M. et al. (2004). ATF4 is a substrate of RSK2 and an essential regulator of osteoblast biology; implication for Coffin-Lowry Syndrome. *Cell* **117**, 387-398.
Yoshida, C. A., Yamamoto, H., Fujita, T., Furuichi, T., Ito, K., Inoue, K., Yamana, K., Zanma, A., Takada, K., Ito, Y. et al. (2004). Runx2 and Runx3 are essential for chondrocyte maturation, and Runx2 regulates limb growth through induction of Indian hedgehog. *Genes Dev.* **18**, 952-963.
Yu, S., Franceschi, R. T., Luo, M., Zhang, X., Jiang, D., Lai, Y., Jiang, Y., Zhang, J. and Xiao, G. (2008). Parathyroid hormone increases activating transcription factor 4 expression and activity in osteoblasts: requirement for osteocalcin gene expression. *Endocrinology* **149**, 1960-1968.
Zhao, M., Sterling, J. A., Qiao, M., Oyajobi, B. O., Harris, S. E. and Mundy, G. R. (2005). The Hedgehog signaling molecule Gli2 regulates both BMP2 and PTHrP expression in the growth plate. *J. Bone Miner. Res.* **20 Suppl. 1**, S40.
Zuscik, M. J., Hilton, M. J., Zhang, X., Chen, D. and O'Keefe, R. J. (2008). Regulation of chondrogenesis and chondrocyte differentiation by stress. *J. Clin. Invest.* **118**, 429-438.